LSST Beam Simulator

J. A. Tyson[1], J. Sasian[2], C. Claver[3], G. Muller[4], K. Gilmore[5], M. Klint[1]
[1]UC Davis, [2]UA Optical Sciences Center, [3]LSST Corp., [4]NOAO, [5]SLAC

Introduction

It is always important to test new imagers for a mosaic camera before device acceptance and constructing the mosaic. This is particularly true of the LSST CCDs due to the fast beam illumination: at long wavelengths there can be significant beam divergence (defocus) inside the silicon because of the long absorption length for photons near the band gap. Moreover, realistic sky scenes need to be projected onto the CCD focal plane. Thus, we need to design and build an f/1.2 re-imaging system. The system must simulate the entire LSST operation, including a sky with galaxies and stars with approximately black-body spectra superimposed on a spatially diffuse night sky emission with its complex spectral features.

The specifications of the LSST beam simulator are to simulate the beam of the LSST telescope, including the obscuration, and to provide a nearly diffraction limited image over a 60 mm diameter field covering an entire 4000x4000 ten micron pixel chip. The FWHM of star images is specified to be 5 microns over several wave-bands (rizy) that need to be imaged. The desired wavelength range is 0.7 to 1.2 micron, but not all at once (allowing refocus in between band changes.) In addition, the system must be compact enabling installation on a laboratory optical table. These specifications are summarized in Table 1.

TABLE 1
LSST Beam Simulator Specifications

• F/1.23 at image
• Image field size 60 mm in diameter
• Magnification = 1.06057
• Total length 665.7 mm
• Diameter 317.5 mm
• Bandwidths: 0.93-1.03; 0.811-0.921; 0.681-0.822 microns in three mechanical positions
• 100 mm diameter obscuration on beam-splitter window

The test stand images a sky scene source which is up to 2m away onto the CCD inside a dewar. All parameters should be tunable over the entire range of LSST operations, including CCD temperature, parallel readout of all segments, readout rate, image dithering, image spectra, filter passbands, sky spectra, etc.

Machining and assembly of the LSST Simulator was done by the NOAO machine and optics shops. Subsequent analysis of CCD images of 5 μm pinholes at various field points was

performed in Feburary, 2011. These analyses have confirmed that the Simulators performance conforms to the listed specifications regarding fraction of enclosed energy and aberration correction, particularly coma and linear astigmatism.

It was possible to achieve the specifications by utilizing a nearly unit magnification system consisting of a spherical mirror, three BK7 lenses, and one beam-splitter window. To achieve the relatively large field the beam-splitter window is used twice and thus the system loses about 80% of the light but this is compensated by the use of brighter sources. Compensation is achieved by moving first lens and reticule relative to the rest of the system.

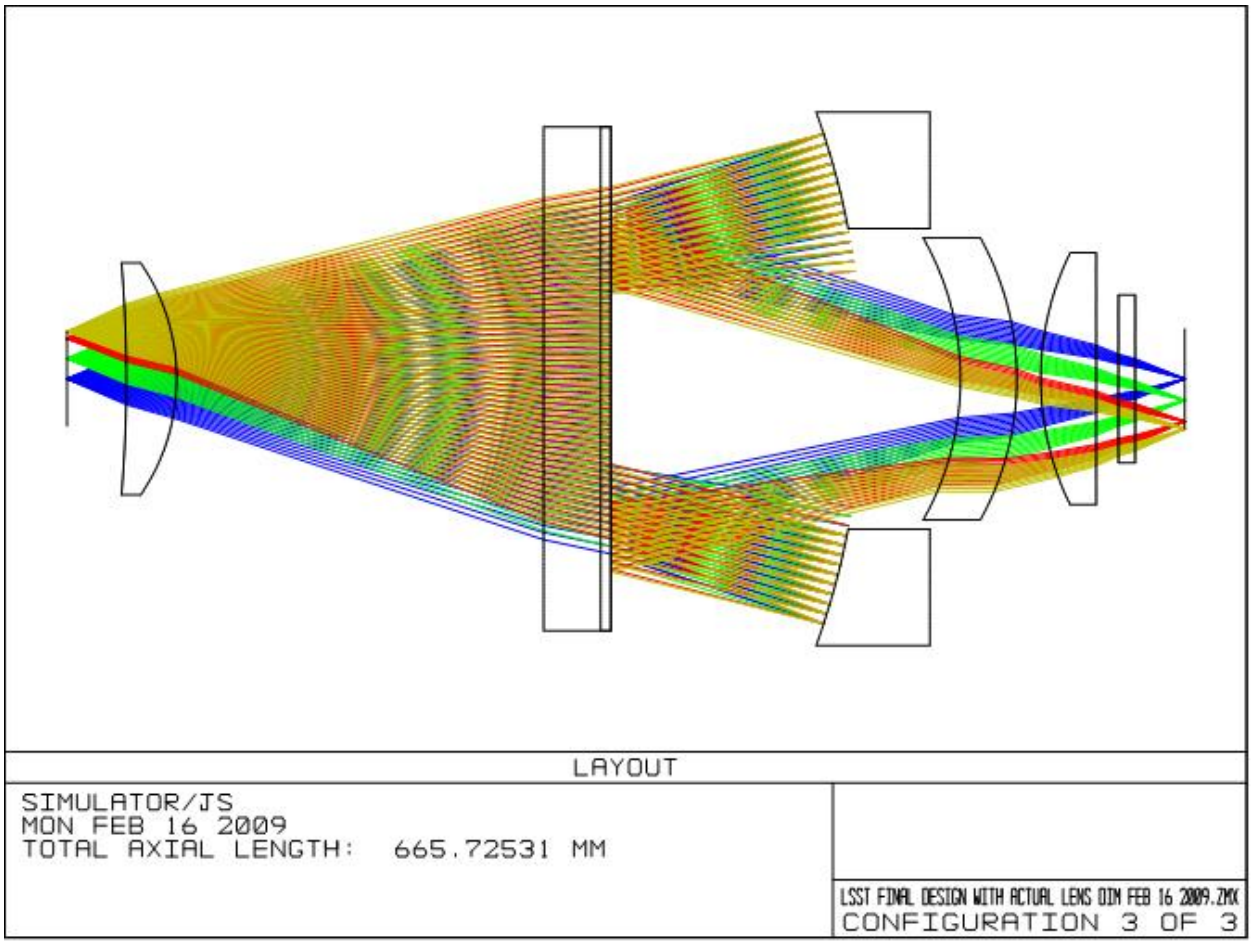

Fig 1. Rays in the double telecentric f/1 reimager, from reticule (left) to focal plane (right).

A variety of optical designs were considered and the final design is shown in Fig. 1. Light from the object on the left side, here a reticule mask with pinholes, reaches the first lens and then 60% of it is transmitted by the beam-splitter. Light then reaches the mirror and is reflected towards the beam-splitter where about 40% is reflected toward the lenses shown on the right side. After light passes through these lenses it enters the cryogenic dewar (not shown here) passing through the quartz dewar window to a focal plane. All lenses and the

dewar window are AR coated and the mirror is aluminum coated. A light baffle in the center of the beam-splitter blocks direct light from reaching the image plane.

The idea of exploiting a spherical mirror and beam-splitter as a unit magnification, high numerical aperture, re-imager can be traced to Burch. The idea of creating a unit magnification system with a spherical mirror is traced to Dyson who introduced further lenses to flatten the field and correct astigmatism. Here both approaches are combined to provide a fast beam over a large field. Other 'lossless' approaches to the problem can become physically large and require many more optical elements and aspheric surfaces.

Analysis of stray light indicates that no significant problems should be expected if proper baffling is integrated into the system. The different wave-bands are accommodated by shifting the first lens and refocusing the reticule mask carrying the array of pinhole stars. The optical length of the system is 665.7 mm and the maximum diameter of the optics is 317.5 mm.

The system should be aligned to the window in tilt since angular misalignment will introduce coma. This is a useful degree of freedom to remove any coma residual in the system. At 0.1 degree of dewar window tilt there is no appreciable change in system performance. The alignment mechanism should provide an angular resolution alignment of at least 0.1 degree in x and y. This must be provided since there can be a small uniform coma residual in the system that can be removed by tilting the system with respect to the dewar window.

While it is possible to get the chip mechanics approximately aligned inside the dewar, there will be tilt errors at the 20 micron/40mm (0.03 deg) level that must be corrected by tilting the dewar once it is cold. We require therefore a way of measuring and adjusting the plane of the as-delivered chip/carrier at room temperature with the dewar open. We want to be able to simulate CCD surface tilt at the level of the camera specs (less than 10 microns / 40mm peak to valley). The dewar manual tilt adjust must thus be 2-axis and cover this range of angles.

Image quality performance

Figure 2 shows the ZEMAX calculated optical performance in the R band (680-820 nm) for a point source. The black line is the diffraction limit, and the three color lines show the performance at various field positions in the focal plane: on-axis (blue), 12mm radius (green), 24mm radius (red), and 28mm radius (yellow). Uniform high quality images are delivered over the entire chip in the focal plane. Half of the energy is enclosed in a 5 micron diameter circle in all bands.

Figure 3 shows the observed fraction of enclosed energy for 5 μm pinholes at 0, 10, 20 and 28 mm radii for the R band (680 – 820 nm). As stated, both field points show half the energy enclosed within a 5 μm diameter.

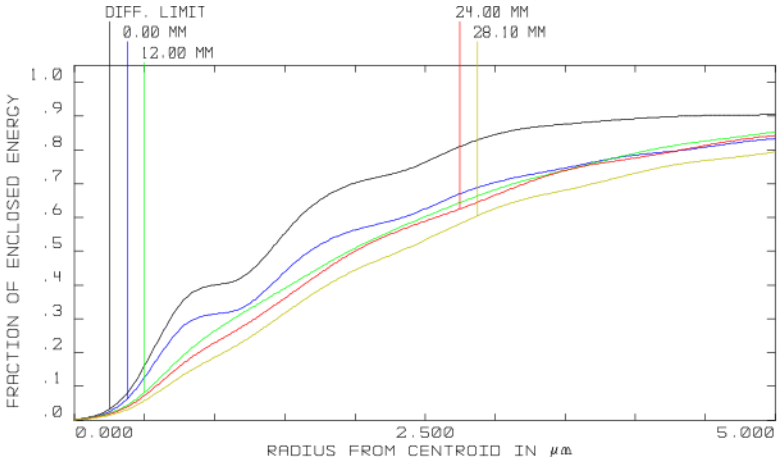

Fig 2. ZEMAZ calculated performance for a point source in the reticule.

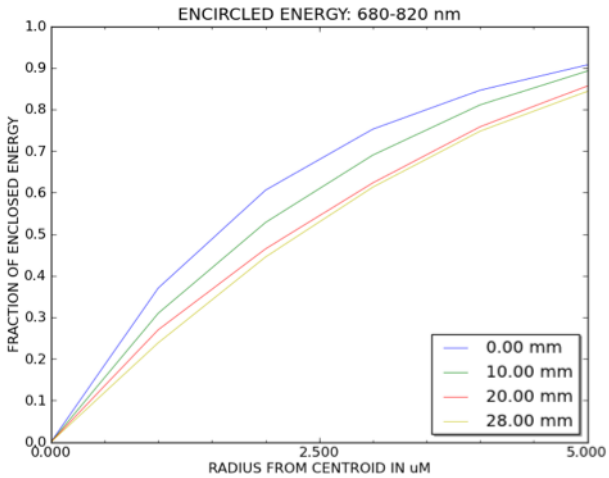

Fig 3. Observed fraction of enclosed energy for a 5 μm pinhole in the reticule.

A de-focused ghost image

Since the system is telecentric, light can be reflected back by the sensor all the way to the spherical mirror and will return almost on its own path to form a second image near the primary image with approximately 0.25 x 0.2 x (sensor reflectivity) = 0.05 x 0.02 reflected light relative to the primary image. However these ghosts are far out of focus, and the spot diagrams of ghost images are larger than 2 mm in diameter, as shown in the following figure. The ghost light is spread over a much larger area than the in-focus PSF by the ratio 3 sq.mm / 20 sq. microns = 1.5e4. So the surface brightness of the ghost is approximately eight orders of magnitude lower than the main in-focus image.

Reflection on the reticule can potentially give a focused ghost image. This is an inherent problem in doubly telecentric systems. The beam splitter window helps to reduce the problem. A large reduction can be obtained via a black non-reflecting coating on the inside surface of the reticule mask.

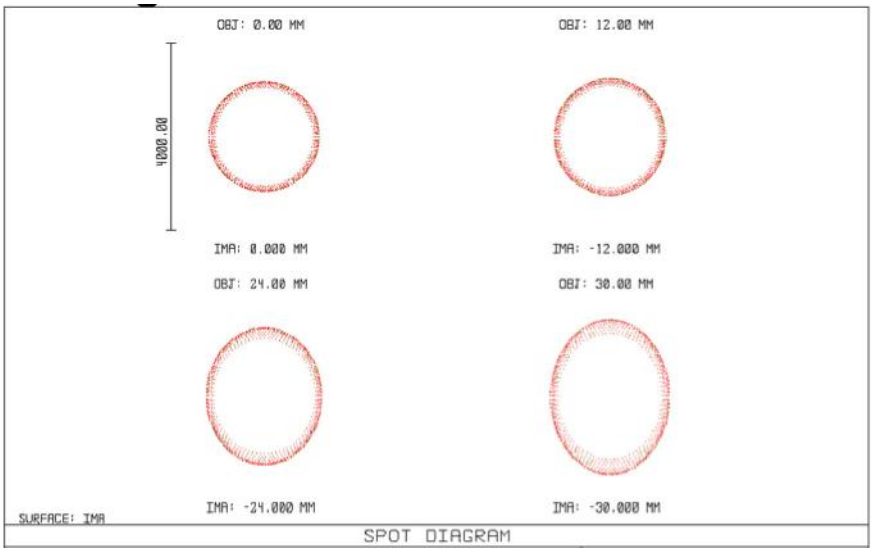

Fig 4. Out of focus 2mm ghost in focal plane due to reflections in the system.

Thus the quality of these expected PSFs are more than sufficient to meet the needs for LSST CCD testing. First, they are totally dominated by diffraction, so any improvements that can be made would be very small. Second, if one convolves these with a 3-5 micron spot (size of the pin hole as the source) the minimal asymmetric effects seen off axis are that much more diluted. The PSF errors will be dominated by the sensor, as intended.

Diffuse night sky simulation

In addition to the stars and galaxies (with their black body spectrum provided by the scattering sphere illumination of the reticule), there is a need to simulate the diffuse night sky and its complex spectrum. This will be done via a spectral engine consisting of a grating, optics, and a MEMS mirror array. The spectral engine will have a 640-1200nm range with 3.7nm FWHM spectral resolution. The complex sky emission spectrum, dominated by multiple vibration-rotation bands, as well as the LSST filter (*rizy*) transmission curve, will be simulated with the spectral engine. Constant illumination over the focal plane is achieved by injecting "sky" light in the pupil plane. Illumination emanating from the periphery of the pupil plane mirror directed towards the splitter mirror will be spread uniformly in the focal plane (Fourier transform of the pupil plane). Four optical fibers arranged around the outside edge of the mirror, aimed upstream towards the back side of the beam splitter mirror will produce the uniform (within 0.5%) illumination across 40x40 mm of the focal plane as seen in the following Figure 5a. Figure 5b shows the orientation of the four fibers with respect to the primary mirror and CCD in the focal plane.

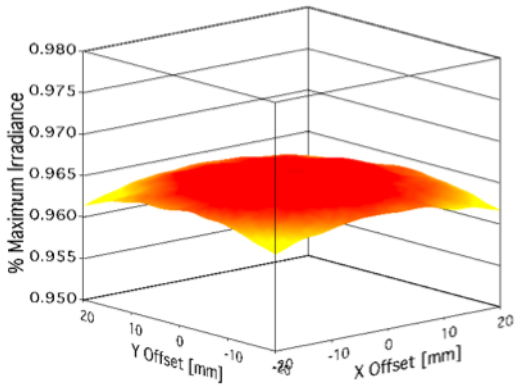

Fig 5a. ZEMAX simulated focal plane irradiance of 4 points sources in the pupil plane.

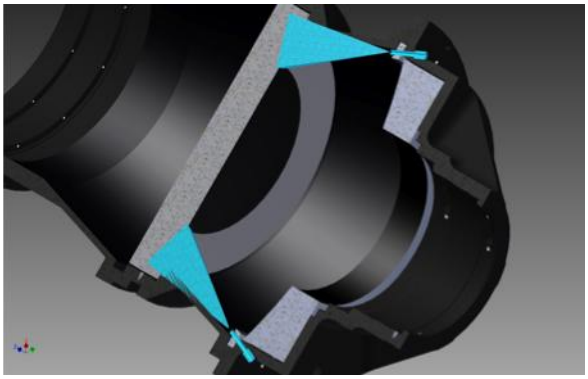

Fig 5b. Cut-away drawing showing fiber optic positioning within the LSST Beam Simulator.

Mechanical system

The optics is held in position with the mechanical assembly shown below in a cut-away drawing. A re-alignment mechanism is integrated with the optical assembly, and baffles are included. The optical assembly will be mounted on a standard optical table, taking

advantage of the modularity and the availability of components the optical table provides at both the input and output ends of the system (shown in drawing below).

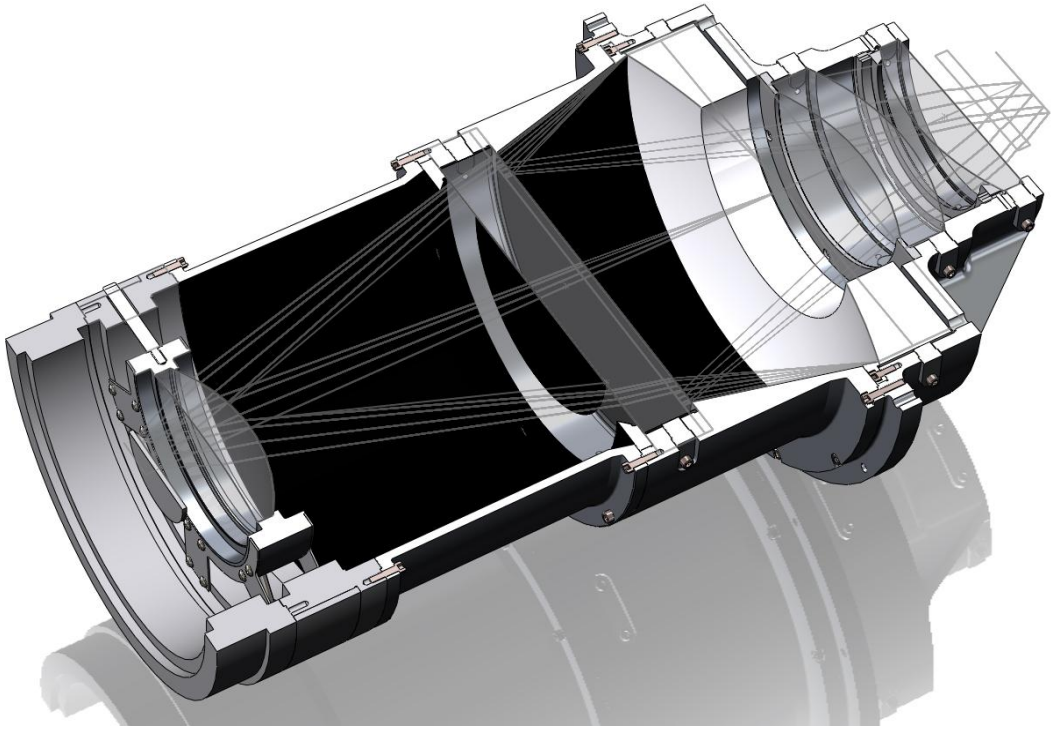

CCD Testing Protocol

The f/1.2 beam setup allows a number of unique tests of the prototype and early delivery science CCDs from vendors. These tests can be divided into several broad classes, depending on different aspects of the CCD response to realistic spectral and spatial illumination, exposure time, clocking rate, and opto-electronic behavior. Wavefront curvature tests and guider tests can also be carried out, starting immediately.

Wavefront sensor tests. In addition to testing the science CCDs, the WFS assembly (including the case where a defocused science 4K CCD is used for WFS) and algorithm can be tested. The wide field with hundreds of stars will enable lab tests of the curvature tomographic inversion algorithm and pipeline. This can be done even before construction using either out-of-focus science CCDs or split CCDs of current design. Controlled aberrations can be introduced and output error signals compared. This can be repeated under a variety of conditions such as vignetting, WFS tilt, star crowding, stellar density, and S/N ratio. This will occur early, before construction, enabling assessment and refinement of the algorithm and optimization of performance under various observing conditions.

Guider tests. The baseline plan for the guide CCDs is to utilize a full 4K science CCD in a "region of interest" mode where fast clocking in two directions is used. This has never been done before, and the analysis of its performance for our segmented thick CCDs assumes no asymmetric systematic such as CTE. The UCD test stand and electronics will allow us to check the performance of these 4K CCDs under this novel application. The performance is expected to depend on the night sky spectral illumination as well as clocking. The test stand permits the appropriate spectral illumination, including night sly emission lines. Since the guider technology decision is in the critical path for the camera, these tests will allow us to examine and hopefully retire this risk on the needed timescale.

Delivered PSF. The response of the device in an f/1.2 beam will vary with wavelength due to optical beam defocus in the thick silicon depletion volume, charge spreading, and CTE. Charge collection and CTE will vary with bias rail voltages. It is possible to have temperature effects as well. Spatial dependence of PSF over the chip will be studied by moving the dewar in x and y with a programmable precision stage. Sensitivity of delivered PSF to optical focal plane and device misalignment as a function of wavelength will also be examined. Pixel-pixel correlation, including noise correlation, will be studied. For some of these tests, a source image consisting of 5 micron holes will be used. Further tests will be performed using realistic delivered optical PSFs (due to expected seeing over a range of 0.4 - 0.7 arcsec, depending on wavelength) utilizing a source mask consisting of realistic 20-35 micron FWHM Gaussian "star" source reticule images. Due to fringing fields, weak lensing shear systematic errors are introduced by non-square effective pixels near the edge of the CCD. This effect will be studied by stepping the illuminating PSF around in the edge area. Finally, the device photometric behavior (especially at 1 micron) as a function of defocus will be studied.

Delivered images. Imaging behavior of detectors depends on details of beam illumination, and device performance. A source mask with a realistic density of stars and galaxies will be used. The spectral energy distribution of these objects will also be realistic, and a true night sky background spectrum will be used. This will test the imaging performance of the CCDs in realistic conditions in the LSST f/1.2 beam. These tests can be done for different clock levels and readout rates examining the S/N for galaxies and stars, in order to validate the LSST choices. Shift-and-stare imaging will be done using the x-y motion of the dewar relative to the beam, and this data will be coadded to search for low level systematics in the CCDs. Finally, the dewar will be misaligned slightly relative to the optical axis in order to introduce a low level of image shear across the CCD, and this will be examined for E-mode and B-mode components as a test of the weak lens performance.

Fringing. At long wavelengths even thick fully depleted CCDs will exhibit some fringing due to narrow night sky emission lines. The realistic sky spectrum generated by the spectral engine enables tests of the fringing in these devices in the f/1.2 LSST beam in a way that cannot be done with tests on other slower beam telescopes or in the lab. Subtle features in CCD response in actual cameras is common, and we need to test these new CCDs in a realistic beam and spectral illumination as soon as possible. This is particularly true of the Y band. The results may impact the camera response model used in ImSim and science capability.

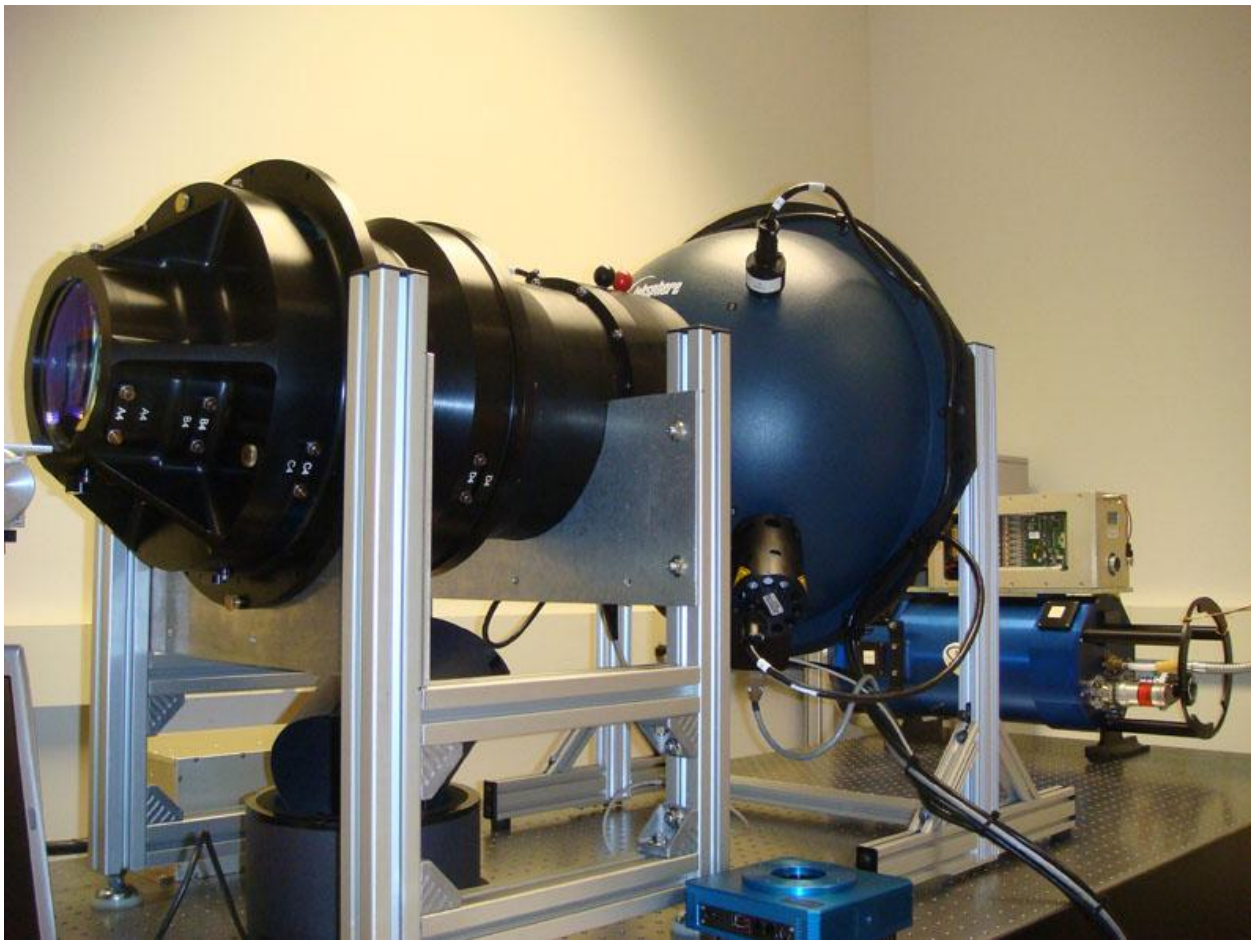

Acknowledgements: We acknowledge support from NSF AST ATI grant 0441069, the W. M. Keck Foundation, Eric Schmidt, and the National Optical Astronomy Observatory.